Effect of Organic Additives or Counterions on the Supramolecular Assembly Structures Constructed by Amphiphiles. A Small-Angle Neutron Scattering Investigation

Toyoko Imae,* Minoru Kakitani, and Motohisa Kato

Faculty of Science, Nagoya University, Nagoya 464, Japan

Michihiro Furusaka

National Laboratory for High Energy Physics, Tsukuba 305, Japan

Received: July 16, 1996; In Final Form: October 10, 1996[⊗]

Small-angle neutron scattering (SANS) was measured for aqueous solutions of amphiphiles with organic additives or counterions such as 2-indenecarboxylic acid, cinnamic acid, and salicylic acid or their ions. The effect of organic species on the supramolecular assembly structure was investigated. Equimolar mixtures of dodecyldimethylamine oxides and aromatic carboxylic acids constructed vesicles. The vesicular bilayer thicknesses were 29−30 Å, independent of organic species. On the other hand, hexadecyltrimethylammoniums with aromatic carboxylate counterions always formed rodlike micelles with axial ratios 8−10. Aqueous solutions of tetradecyltrimethylammonium salicylate displayed a strong interparticle interference effect on SANS profiles at concentrations above 0.8×10^{-2} g cm^{-3}, although such an effect disappeared with addition of more than 5/mM sodium salicylate.

Introduction

When organic additives are added to aqueous solutions of amphiphiles, they are solubilized into the supramolecular assemblies and sometimes modify the assembly structures. It is also known that the structures of supramolecular assemblies constructed by ionic amphiphiles depend on counterion species, especially the organic counterions effect on the assembly structures stronger than inorganic counterions such as chloride and bromide.

A weak base amphiphile, dodecyldimethylamine oxide (C_{12}DAO), forms spherical micelles in water.[1] Although the addition of NaCl did not increase the micellar aggregation number so as to change the structure, aqueous C_{12}DAO solutions with additional hexanol displayed vesicular, lamellar, and bicontinuous phases, depending on the mixing ratio.[2,3] This indicates bilayer formation by C_{12}DAO coupled with hexanol. The bilayer arrangement was also confirmed in aqueous C_{12}DAO solutions mixed with cinnamic acid.[4,5] Vesicles were constructed above a threshold mixing ratio, and the multilamellar layers in vesicles were most predominant at equimolar mixing.

Aromatic carboxylate counterions on cationic micelles behave differently from aromatic carboxylic acids mixed in aqueous C_{12}DAO solutions. While aqueous solutions of alkylpyridinium halides and alkyltrimethylammonium (C_nTA) halides were fluid, solutions of hexadecylpyridinium salicylate (C_{16}PySal) and alkyltrimethylammonium salicylate (C_nTASal, $n = 14, 16$) were viscous, viscoelastic, and spinnable.[6−10] The difference in rheological behavior is due to the micellar structures, that is, whether spherical or rodlike, as confirmed by micellar aggregation numbers.[11−13] The formation of rod in water was also verified for hexadecyltrimethylammonium 2-indenecarboxylate (C_{16}TAIn) micelles,[14] although the aggregation number of hexadecyltrimethylammonium bromide (C_{16}TAB) micelles increased only 3 times by adding 0.08 M octylamine against 0.1 M C_{16}TAB.[15] On the other hand, tetradecylpyridinium *n*-heptanesulfonate displayed a sphere to rod transition at the threshold micelle concentration.[16]

In this position, we do not know whether the formation of vesicles and rodlike micelles in aqueous amphiphile solutions with organic species originates in amphiphiles or organic species. Therefore, in this work, the supramolecular assembly structures constructed in aqueous solutions of C_{12}DAO with different aromatic acids and of C_{16}TA with different aromatic counterions are investigated by small-angle neutron scattering (SANS) and light scattering. The contribution of aromatic species in the construction of different supramolecular structures is discussed. A SANS measurement is also carried out for aqueous C_{14}TASal solutions at different C_{14}TASal and sodium salicylate (NaSal) concentrations. The interaction between supramolecules is discussed.

Experimental Section

C_{12}DAO ($C_{12}H_{25}N(CH_3)_2O$) was purchased from Fulka Co. Ltd. and used without further purification. 2-Indenecarboxylic acid (C_9H_7COOH), salicylic acid ($C_6H_4(OH)COOH$), and sodium salicylate ($C_6H_4(OH)COONa$) were commercial products. C_{16}TACin ($C_{16}H_{33}N^+(CH_3)_3C_6H_5CH{=}CHCOO^-$) and C_{14}TASal ($C_{14}H_{29}N^+(CH_3)_3C_6H_4(OH)COO^-$) were prepared by exchanging inorganic ions of C_nTACl into cinnamate and salicylate ions, respectively.[9] H_2O as a solvent of light scattering was redistilled from alkaline KM_nO_4. Commercial D_2O was used as a solvent of SANS.

Equimolar mixtures of C_{12}DAO with 2-indenecarboxylic acid and salicylic acid in water were prepared at a concentration of 0.2×10^{-2} g cm^{-3} (0.2%). While a concentration of aqueous C_{16}TACin solution was 0.2×10^{-2} g cm^{-3}, aqueous C_{14}TASal solutions were prepared at several C_{14}TASal and NaSal concentrations. Aqueous solutions of C_{16}TACin and C_{14}TASal were clear, whereas aqueous solutions of C_{12}DAOIn and C_{12}DAOSal were opalescent as well as C_{12}DAOCin.[5]

The light scattering and specific refractive index increment were measured at 25 °C on an Otsuka Electric DLS 700 spectrophotometer and an RM-102 differential refractometer,

* Corresponding author. Tel 052-789-2483; FAX 052-789-2962; e-mail imae@chem2.chem.nagoya-u.ac.jp.

[⊗] Abstract published in *Advance ACS Abstracts,* December 1, 1996.

S0022-3654(96)02127-2 CCC: $12.00

TABLE 1: Characteristics of Supramolecular Assemblies in Aqueous Amphiphile Solutions with Organic Additives or Counterions

	LS						SANS		
sample	$\partial n/\partial c$,cm^3 g^{-1}	M,10^5	m	R_G, Å	R_H, Å	ρ	$t/2$, Å	R_t, Å	L, Å
C_{12}DAOIn	0.205	193	49 600	809	1040	0.78	14.9		
C_{12}DAOCin[a,b]	0.170	500	132 000	964	1010	0.95	15		
C_{12}DAOSal							14.7		
C_{16}TAIn[a]	0.198	2.7	609		102				400
C_{16}TACin	0.223	2.3	534		126			25.2	600
C_{16}TASal[c]	0.177	3.7	880						

[a] References 4 and 14. [b] Reference 5. [c] Reference 12.

respectively. An argon ion laser of 488 nm wavelength was used as a light source, and the scattering angle was changed from 30° to 150°. A 10 mm diameter quartz cell was used.

SANS measurements were carried out on a cold neutron small-angle scattering instrument SAN at the National Laboratory for High Energy Physics (KEK). The instrument was operated at a neutron radiation of 1−16 Å wavelength at room temperature (~25 °C). The scattering vector amplitude Q range was 0.008−0.2 Å^{-1}. A rectangular quartz cell of dimensions 22 × 40 × 2 mm was used. The scattering intensity was corrected for intensities of back ground and empty cell.[17,18] Then the intensity in absolute units was calculated by using scattering from H_2O in a 1 mm cell.

Results and Discussion

Light Scattering. Light scattering intensity measurements at different scattering angles were carried out for aqueous C_{12}DAOIn and C_{16}TACin solutions of 0.2 × 10^{-2} g cm^{-3}. The refractive index increment $\partial n/\partial c$ was 0.205 and 0.223 cm^3 g^{-1}, respectively. The critical micelle concentration c_0 utilized for calculation was 0.021 and 0.059 × 10^{-2} g cm^{-3}, respectively. From the static light scattering, the molecular weight M and radius of gyration R_G were calculated according to the equation

$$K(c - c_0)/\Delta R_\theta = (1 + R_G^2 Q^2/3)/M + 2B(c - c_0) \quad (1)$$

where K is the optical constant, c is the amphiphile concentration, and ΔR_θ is the reduced scattering intensity difference at scattering angle θ. B is the second virial coefficient. The second term on the right side of the equation was neglected because the amphiphile concentration was very low. The evaluated M, R_G, and aggregation number m are listed in Table 1 with the refractive index increment. The scattering angle dependence was too small to calculate the R_G value for C_{16}TACin.

The hydrodynamic radius R_H was calculated from dynamic light scattering on the basis of the equation

$$D_c = (k_B T/6\pi\eta_0 R_H)[1 + k_D(c - c_0)] \quad (2)$$

where D_c is the diffusion coefficient extrapolated to zero scattering angle, k_B is the Boltzmann constant, T is the absolute temperature, η_0 is the viscosity of the solvent, and k_D is the hydrodynamic virial coefficient. The D_c values were obtained as average of values measured at low angles (20° − 30°). The virial term was neglected. Table 1 lists the calculated values as well as numerical values for C_{12}DAOCin, C_{16}TAln, and C_{16}TASal molecular assemblies obtained previously.[4,5,12,14]

The aggregation number of supramolecular assemblies in opalescent C_{12}DAOIn solution was as large as 49 600 as well as that for C_{12}DAOCin which forms vesicles.[4,14] The ratio ρ (=R_G/R_H) was close to or less than unity.[19] These results indicate that, in C_{12}DAO solutions with aromatic carboxylic acid, vesicles are formed rather than rodlike micelles. On the other hand, the aggregation number of C_{16}TACin assembly was as small as 534. Similar aggregation numbers were obtained in aqueous C_{16}TAIn and C_nTASal solutions,[12−14] indicating the formation of rodlike micelles.

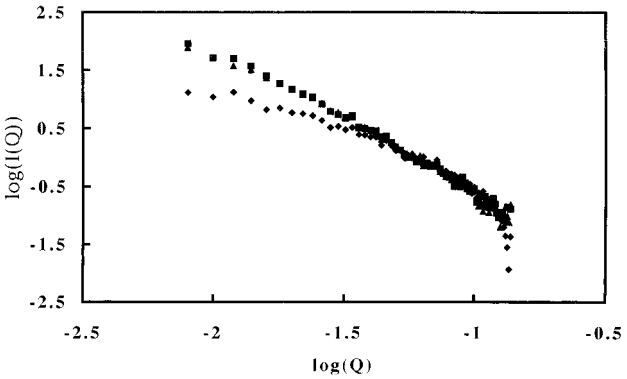

Figure 1. SANS data for aqueous amphiphile solutions of 0.2 × 10^{-2} g cm^{-3}: (▲) C_{12}DAOIn, (■) C_{12}DAOSal, (◆) C_{16}TACin.

SANS for Aqueous C_{12}DAOIn, C_{12}DAOSal, and C_{16}TACin Solutions. Figure 1 shows double-logarithmic plots of SANS intensity $I(Q)$ versus scattering vector amplitude Q for aqueous C_{12}DAOIn, C_{12}DAOSal, and C_{16}TACin solutions of 0.2 × 10^{-2} g cm^{-3}. SANS profiles for C_{12}DAOIn and C_{12}DAOSal were very similar. With increase in Q, their scattering intensities decreased more than the intensities for C_{16}TACin. Since a vesicular supramolecular assembly structure can be assumed for C_{12}DAOIn and C_{12}DAOSal, as described above, their SANS data were treated with the same analytical procedure applied to C_{12}DAOCin vesicles.[5]

When the theoretical equation for vesicular structure[5,17,18] is applied to the SANS data for aqueous C_{12}DAOIn and C_{12}DAOSal solutions, the $Q^2I(Q)$ values must be independent of Q^2 values. However, the experimental data were not such a case. This means that vesicles are too large to estimate the whole size from SANS. Then a periodic multilamellar structure of large vesicles with infinitely extended bilayers is analyzed on the basis of the equation[20]

$$Q^2 I(Q) = (2\pi t^2/D)(\rho - \rho_s)^2[\sin(Qt/2)/(Qt/2)]^2 \quad (3)$$

where t is the width of the scattering length density profile and D is the repeat distance of the bilayers. $\rho - \rho_s$ is the mean coherent neutron scattering length density difference between assembly and solvent.

Equation 3 was applied to C_{12}DAOIn and C_{12}DAOSal vesicles, and the optimum bilayer thicknesses were calculated as 29.8 and 29.4 Å, respectively. The optimum fitting curves are shown in Figure 2. When numerical values of bilayer thicknesses are compared with that of C_{12}DAOCin vesicles[5] (see Table 1), it can be concluded that bilayer thicknesses of C_{12}DAO vesicles with aromatic additives (Ar) are common, indicating the similarity of the adsorption of additives. How-

ever, the thickness of about 30 Å is too short in comparison with twice the molecular length and diameter of spherical C_{12}DAO micelles.[5] This indicates that organic additives must penetrate into bilayers and alkyl chains must be in tilt, melt, or comb shape, as illustrated in Figure 3. From SANS measurements, Baumann et al.[21] determined bilayer thickness of lamellar layers formed in quaternary solutions of tetradecyltrimethylamine oxide, decane, hexanol, and D_2O. The thicknesses were larger than twice the molecular length, because decane located in between bilayers.

Supramolecular assemblies of C_{16}TA with organic counterions were assumed to be rodlike micelles with aggregation numbers of 500−900 as described above. If particles take a cylindrical structure of length L and transverse cross-sectional radius R_t, the SANS intensity is written by[17,18]

$$QI(Q) = \pi n_p L A_t^2 (\rho - \rho_s)^2 [2j_1(QR_t)/QR_t]^2$$

$$j_1(QR_t) = [\sin(QR_t) - (QR_t)\cos(QR_t)]/(QR_t)^2 \qquad (4)$$

when L is fairly long in comparison to R_t, where n_p is the number density of supramolecular assemblies, and $A_t = \pi R_t^2$ is the transverse cross-sectional area. The calculated numerical values based on eq 4 were fitted to the observed data, and the optimum radius of 25.2 Å for C_{16}TACin rods was obtained, as listed in Table 1. The fitting curve is illustrated in Figure 2. The calculated radius was consistent with the theoretical molecular length.

The hydrodynamic radius of rigid rod with length L and cross-sectional radius R_t can be calculated from the equation[22]

$$R_H = L[2\ln(L/R_t) - 0.19 - 8.24/\ln(L/R_t) + 12/\{\ln(L/R_t)\}^2]^{-1} \qquad (5)$$

When the rod radius R_t value of 25.2 Å calculated from SANS analysis and the hydrodynamic radius R_H obtained from light scattering were utilized, the rod lengths of 600 and 400 Å for C_{16}TACin and C_{16}TAIn, respectively, were evaluated. Then, the ratio of $L/2R$ was 8−12, indicating the formation of rods with axial ratio of about 10 in aqueous solutions of hexadecyltrimethylammonium with aromatic counterion ($C_{16}TA^+Ar^-$) (see Figure 3). The numerical values are listed in Table 1. The formation of rod with similar size was already reported for aqueous C_nTASal and C_{16}PySal solutions.[11−13]

SANS for Aqueous C_{14}TASal Solutions with and without NaSal. Figures 4 and 5 show SANS intensities $I(Q)$ as a function of scattering vector amplitude Q for aqueous C_{14}TASal solutions of different C_{14}TASal concentrations. Scattering intensities decreased monotonously with increasing Q at concentrations of 0.2 and 0.5 × 10^{-2} g cm^{-3}. Above 0.8 × 10^{-2} g cm^{-3}, intensities had maximum which shifted to higher Q values with concentration. This indicates that the interaction between assemblies increases. The NaSal concentration dependence on SANS intensities is also given in Figure 4. The maximum profile in SANS intensities diminished with adding NaSal, and intensities decreased monotonously with Q for solutions with 0.005 and 0.1 M NaSal, suggesting the decrease in the interaction between assemblies, although intensities for a solution with 1 M NaSal was very weak.

Supposing an isotropic ensemble of identical particles, the SANS intensity $I(Q)$ is approximated as[17,18]

$$I(Q) = n_p P(Q)\, S(Q) = I(Q)'\, S(Q) \qquad (6)$$

where $P(Q)$ is the intraparticle structure factor which depends on the particle geometry, and $S(Q)$ is the interparticle structure factor which is related to the interparticle interaction potential through the radial distribution function. Since $S(Q)$ can be

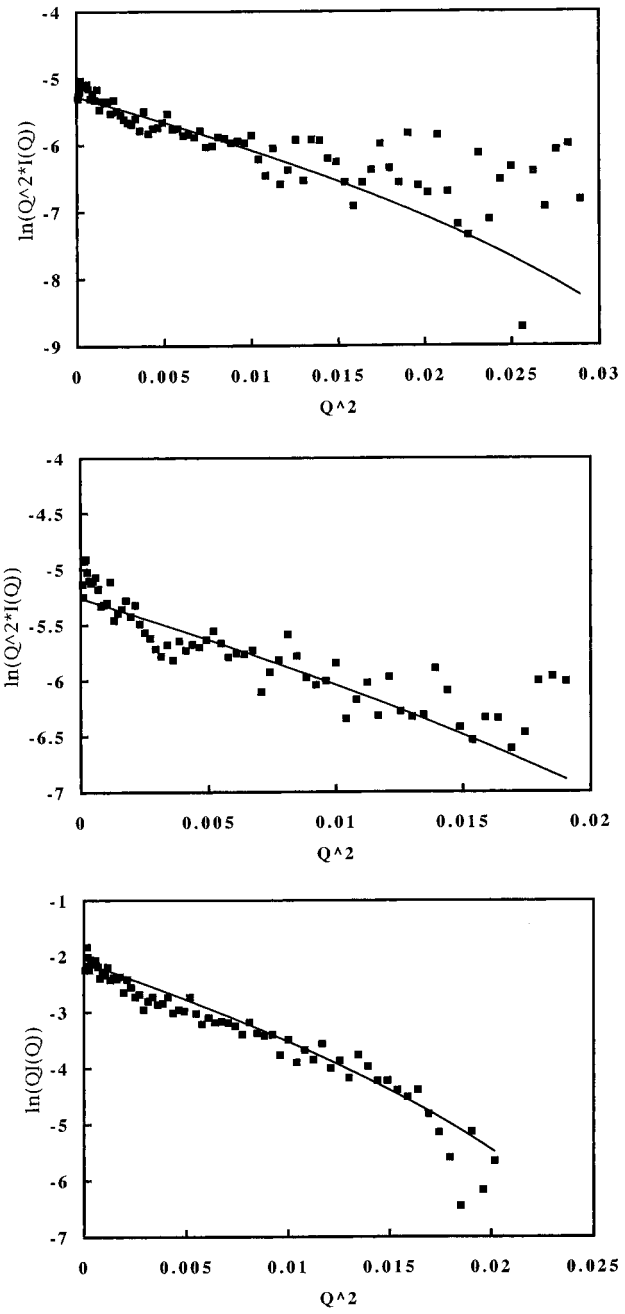

Figure 2. SANS data for aqueous amphiphile solutions of 0.2 × 10^{-2} g cm^{-3}: (■) observed data; (—) calculated curves. Top, C_{12}DAOIn; middle, C_{12}DAOSal; bottom, C_{16}TACin.

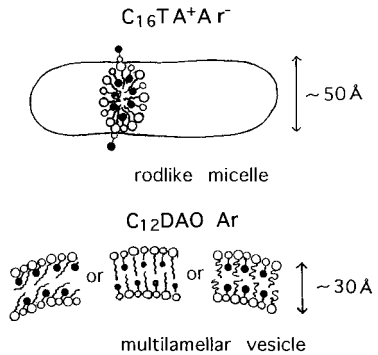

Figure 3. Schematic models of supramolecular assembly structure of amphiphiles with organic additives and counterions.

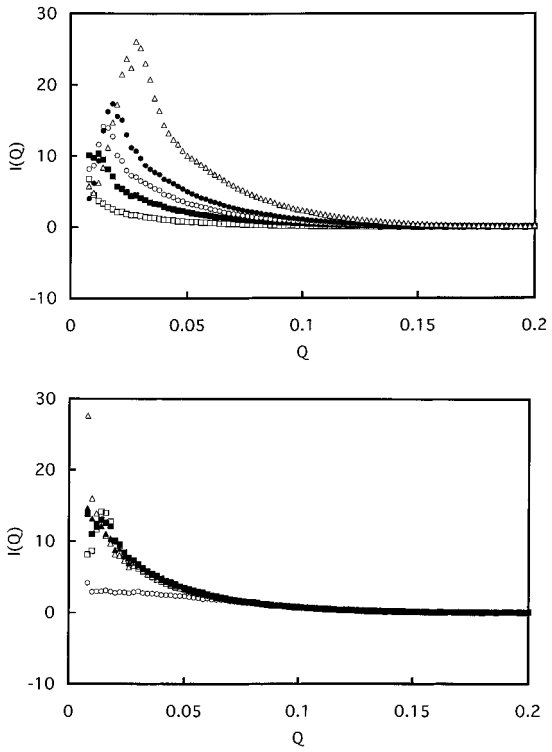

Figure 4. SANS data for aqueous C_{14}TASal solutions. (top) Amphiphile concentration (10^{-2} g cm^{-3}) dependence on solutions without NaSal: (□) 0.2, (■) 0.5, (○) 0.8, (●) 1.3, (△) 2.0. (bottom) NaSal concentration C_{NaSal} (M) dependence on solutions of 0.8×10^{-2} g cm^{-3}: (□) 0, (■) 0.001, (▲) 0.005, (△) 0.1, (○) 1.

approximated to be unity for dilute solutions, this term was left out of consideration in the analysis described above. However, it has a meaningful contribution for concentrated C_{14}TASal solutions above 0.8×10^{-2} g cm^{-3}. Then, for the rod structure, $I(Q)$ in eq 4 must be rewritten as $I(Q)'$ of eq 6.

The procedure explained now was applied to SANS data for aqueous C_{14}TASal solutions with and without NaSal as shown in Figures 4 and 5. Evaluated cross-sectional radii of rods were listed in Table 2. Since the supramolecular assembly in a C_{14}TASal solution of 0.8×10^{-2} g cm^{-3} with 1 M NaSal was confirmed to be spherical micelles from light scattering experiment,[13] the equation[17,18]

$$I(Q) = n_p V^2(\rho - \rho_s)^2[3j_1(QR)/QR]^2 \qquad (7)$$

was used instead of eq 4, where $V = 4\pi R^3/3$ and R are volume and radius, respectively, of spherical micelles. The evaluated radius was included in Table 2. Radii of rodlike and spherical micelles were consistent with molecular length, almost independent of C_{14}TASal and NaSal concentrations. $I'(Q)$ and $S(Q)$ curves for solutions of 2×10^{-2}, 4×10^{-2}, and 6×10^{-2} g cm^{-3} are illustrated in Figure 5. While $I'(Q)$ curves monotonously decreased with increasing Q, $S(Q)$ curves had maximum and constricted to unity as expected.

The contribution of intermicellar correlation was reported for aqueous solutions of sodium dodecyl sulfate (SDS),[23] lithium dodecyl sulfate (LDS),[24] hexadecyltrimethylammonium chloride,[25] and sodium *p*-(1-pentylheptyl)benzenesulfonate.[26] However, the amphiphile concentrations where the intermicellar correlation occurred were about 1 order higher in those systems than in aqueous C_{14}TASal solutions. The occurrence of intermicellar correlation at concentrations comparable to those for C_{14}TASal was reported for aqueous solutions of C_{16}PySal[11] and sodium dodecyl-*o*-xylenesulfonate.[27] The rod length and the correlation increased with C_{16}PySal concentration. The

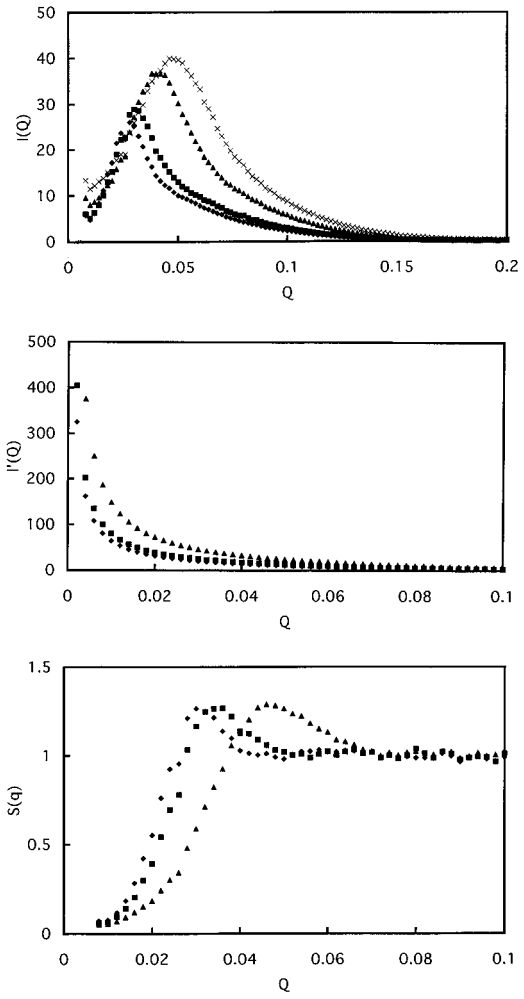

Figure 5. SANS data for aqueous C_{14}TASal solutions. (top) $I(Q)$ vs Q; (middle) $I'(Q)$ vs Q; (bottom) $S(Q)$ vs Q. Amphiphile concentration (10^{-2} g cm^{-3}): (◆) 2, (■) 4, (▲) 6, (×) 10.

TABLE 2: Characteristics of Supramolecular Assemblies in Aqueous C_{14}TASal Solutions

C_{NaSal}, M	c, 10^{-2} g cm^{-3}	R_t, Å	R, Å
0	0.2	25.5	
	0.5	21.5	
	0.8	23.0	
	1.3	23.0	
	2.0	21.8	
	4.0	21.7	
	6.0	21.3	
	10.0	19.4	
0	0.8	23.0	
0.001		22.0	
0.005		21.9	
0.1		21.7	
1			24.0

intermicellar correlation was significant in the range of sodium dodecyl-*o*-xylenesulfonate concentrations from 0.25 to 5 wt %.

The origin of the interparticle interaction for ionic particles is mainly the electrostatic repulsion. According to the DLVO theory, the electrostatic, repulsive interaction potential depends on ionic strength of a solution and surface potential of particle.[19] Low ionic strength and high charge number increase the interaction potential. In micellar solutions without additive salt, ionic strength originates in free monomeric molecules, that is, critical micelle concentration (cmc). The cmc for aqueous C_{14}TASal solution was as low as 1 mM,[13] which was 1 order of magnitude lower than that of regular ionic micelles such as LDS micelles.[24] As a result, low ionic strengths in aqueous

C_{14}TASal solutions induce the strong intermicellar correlation. The positive surface charge on rodlike C_{14}TASal micelles in water was confirmed by electrophoretic mobility measurement.[13] Then the surface potential of C_{14}TASal micelles in water at 25 °C calculated from electrophoretic mobility 2.77×10^{-4} cm^2 V^{-1} s^{-1} is 53 mV. Since this value is comparable to values for SDS micelles,[28] the electrostatic interaction potential between C_{14}TASal micelles is contributed from surface potential as well as between spherical ionic micelles. Similar discussion is valid for rodlike micelles of C_{16}TASal, C_{16}PySal, and sodium dodecyl-*o*-xylenesulfonate. C_{16}TASal micelles in water had a lower cmc and higher electrophoretic mobility or surface potential than C_{14}TASal micelles.[12] For rodlike C_{16}PySal micelles with around 500 Å length, the cmc was as low as 0.15 mM, although the degree of dissociation determined from conductivity measurement was less than 10%.[29] On the other hand, the cmc of ellipsoidal micelles of sodium dodecyl-*o*-xylenesulfonate with axial ratio less than 2 was 0.5−2.5 mM, depending on temperature, and their fractional charge was 0.18−0.23.[27]

The intermicellar correlation was also observed for light scattering of aqueous C_nTASal solutions.[12,13] The minimum C_{14}TASal or NaSal concentrations where the intermicellar correlation occurred or vanished, respectively, were consistent with those observed from SANS in the present work. The intermicellar correlation disappeared at NaSal concentrations above 5 and 1 mM for 20 mM C_{14}TASal and 5 mM C_{16}TASal solutions, respecitvely. Bendedouch et al.[24] reported the effect of salt on the intermicellar correlation in aqueous LDS solutions. Although the correlation diminished with addition of LiCl and the effect depended on LDS concentration, salt concentration necessary for vanishing intermicellar correlation was rather high in comparison with that in aqueous C_nTASal solutions. Even 1 M LiCl was not sufficient to screen completely the electrostatic repulsion between micelles in 0.147 M LDS solutions. This can be ascribed to the strong adsorption ability of salicylate ions. The charge signs of C_{14}TASal micelles were reversed at 0.1 M NaSal concentration by the penetration of salicylate ions in micelles.[13] This phenomenon has never observed by inorganic counterions.

Aqueous C_nTASal solutions as well as C_nPySal solutions displayed strong viscoelasticity and spinnability.[6−10] The characteristic rheological properties were stronger at higher concentration but diminished with addition of NaSal above 2 and 5 mM for C_{14}TASal and C_{16}TASal micelles, respectively, although a second maximum of rheological parameters appeared at 0.1 M NaSal. The NaSal effect on rheology is indirectly related to the effect for electrostatic interaction potential but not directly, because repulsive interaction, in effect, is contrary to rheology. Therefore, the specific, strong attractive interaction must exist at extremely close intermicellar distances in aqueous C_nTASal solutions without or with less NaSal.

Acknowledgment. The authors are grateful to Mr. O. Mori, Mr. Y. Kuwahara, and Miss K. Fujita for their assistance in SANS and light scattering measurements. We also thank Prof. K. Takagi for valuable discussion about this subject.

References and Notes

(1) Ikeda, S.; Tsunoda, M.; Maeda, H. *J. Colloid Interface Sci*. **1979**, *70*, 448.
(2) Hoffmann, H.; Thunig, C.; Schmiedel, P.; Munkert, U. *Nuovo Cimento* **1994**, *16*, 1373.
(3) Imae, T.; Iwamoto, T.; Platz, G.; Thunig, C. *Colloid Polym. Sci.* **1994**, *272*, 604.
(4) Imae, T.; Tsubota, T.; Okamura, H.; Mori, O.; Takagi, K.; Itoh, M.; Sawaki, Y. *J. Phys. Chem*. **1995**, *99*, 6046.
(5) Okamura, H.; Imae, T.; Takagi, K.; Sawaki, Y.; Furusaka, M. *J. Colloid Interface Sci*. **1996**, *180*, 98.
(6) Hoffmann, H.; Platz, G.; Rehage, H.; Schorr, W. *Adv. Colloid Interface Sci.* **1982**, *17*, 275.
(7) Rehage, H.; Wunderlich, I.; Hoffmann, H. *Prog. Colloid Polym. Sci.* **1986**, *72*, 51.
(8) Imae, T.; Hashimoto, K.; Ikeda, S. *Colloid Polym. Sci*. **1990**, *268*, 460.
(9) Hashimoto, K.; Imae, T.; Nakazawa, K. *Colloid Polym. Sci*. **1992**, *270*, 249.
(10) Imae, T. *Colloids Surf. A* **1996**, *109*, 291.
(11) Kalus, J.; Hoffmann, H.; Reizlein, K.; Ulbricht, W.; Ibel, K. *Ber. Bunsen-Ges. Phys. Chem*. **1982**, *86*, 37.
(12) Imae, T. *J. Phys. Chem.* **1990**, *94*, 5953.
(13) Imae, T.; Kohsaka, T. *J. Phys. Chem*. **1992**, *96*, 10030.
(14) Imae, T.; Mori, O.; Takagi, K.; Itoh, M.; Sawaki, Y. *Colloid Polym. Sci*. **1995**, *273*, 579.
(15) Prasad, Ch. D.; Singh, H. N. *J. Colloid Interface Sci.* **1993**, *155*, 415.
(16) Hoffmann, H.; Rehage, H.; Platz, G.; Schorr, W.; Thurn, H.; Ulbricht, W. *Colloid Polym. Sci.* **1982**, *260*, 1042.
(17) Chen, S. H. *Annu. Rev. Phys. Chem.* **1986**, *37*, 351.
(18) Chen, S. H.; Lin, T. L. *Methods Exp. Phys.* **1987**, *23*, 489.
(19) Van De Sandre, W.; Persoons, A. *J. Phys. Chem*. **1985**, *89*, 404.
(20) Strey, R.; Schomacker, R.; Roux, D.; Nallet, F.; Olsson, U. *J. Chem. Soc., Faraday Trans.* **1990**, *86*, 2253.
(21) Baumann, J.; Kalus, J.; Hoffmann, H.; Thunig, C.; Lindner, P. *Ber. Bunsen-Ges. Phys. Chem*. **1991**, *95*, 795.
(22) Newman, J.; Swinney, H. L.; Day, L. A. *J. Mol. Biol*. **1977**, *116*, 593.
(23) Hayter, J. B. *Ber. Bunsen-Ges. Phys. Chem*. **1981**, *85*, 887.
(24) Bendedouch, D.; Chen, S.-H.; Koehler, W. *J. Phys. Chem.* **1983**, *87*, 2621.
(25) Hayter, J. B.; Penfold, J. *Colloid Polym. Sci.* **1983**, *261*, 1022.
(26) Triolo, R.; Hayter, J. B.; Magid, L. J.; Johnson, Jr., J. S. *J. Chem. Phys*. **1983**, *79*, 1977.
(27) Sheu, E. Y.; Chen, S. H.; Huang, J. S. *J. Phys. Chem.* **1987**, *91*, 1535.
(28) Kameyama, K.; Takagi, T. *J. Colloid Interface Sci*. **1990**, *140*, 517.
(29) Hoffmann, H.; Platz, G.; Rehage, H.; Schorr, W.; Ulbricht, W. *Ber. Bunsen-Ges. Phys. Chem*. **1981**, *85*, 255.

JP962127+